ISSN 0020-1685, Inorganic Materials, 2020, Vol. 56, No. 8, pp. 854–858. © Pleiades Publishing, Ltd., 2020.
Russian Text © The Author(s), 2020, published in Neorganicheskie Materialy, 2020, Vol. 56, No. 8, pp. 901–905.

Synthesis, Structure, and Thermophysical Properties of $EuGaGe_2O_7$

L. T. Denisova[a, *], M. S. Molokeev[b, c], L. A. Irtyugo[a], V. V. Beletskii[a], Yu. F. Kargin[d], and V. M. Denisov[a]

[a] *Institute of Nonferrous Metals and Materials Science, Siberian Federal University, Svobodnyi pr. 79, Krasnoyarsk, 660041 Russia*

[b] *Kirensky Institute of Physics, Krasnoyarsk Scientific Center Federal Research Center, Siberian Branch, Russian Academy of Sciences, Akademgorodok 50/38, Krasnoyarsk, 660036 Russia*

[c] *Institute of Engineering Physics and Radio Electronics, Siberian Federal University, ul. Akademika Kirenskogo 28/12(B), Krasnoyarsk, 660041 Russia*

[d] *Baikov Institute of Metallurgy and Materials Science, Russian Academy of Sciences, Leninskii pr. 49, Moscow, 119991 Russia*

**e-mail: antluba@mail.ru*

Received December 16, 2019; revised January 23, 2020; accepted February 4, 2020

Abstract—The europium gallium germanate $EuGaGe_2O_7$ has been prepared by solid-state reaction in air in the temperature range 1273–1473 K using a stoichiometric mixture of Eu_2O_3, Ga_2O_3, and GeO_2. Its crystal structure has been determined by X-ray diffraction (sp. gr. $P2_1/c$, a = 7.1693(7) Å, b = 6.57008(6) Å, c = 12.7699(1) Å, β = 117.4522(5)°, V = 533.768(8) Å^3). The heat capacity of polycrystalline samples has been determined by differential scanning calorimetry in the temperature range 350–1053 K and the experimental data have been used to calculate the thermodynamic properties (enthalpy increment, entropy change, and reduced Gibbs energy change) of $EuGaGe_2O_7$.

Keywords: europium gallium germanate, solid-state synthesis, differential scanning calorimetry, heat capacity, structure, thermodynamic properties

DOI: 10.1134/S002016852008004X

INTRODUCTION

Researchers' interest in the mixed oxide compounds with the general formula $RMGe_2O_7$ (R = rare-earth metal; M = Al, Ga, In, Fe) is aroused by their potential practical applications [1–8]. The $RMGe_2O_7$ (M = Al, Ga) germanates have a monoclinic structure (sp. gr. $P2_1/c$), whereas the space group of the $RFeGe_2O_7$ compounds depends on the ionic radius of the rare-earth ions: $P2_1/c$ for La–Gd and $P2_1/m$ for Tb–Lu [7–9]. The least studied germanates include the $RGaGe_2O_7$ compounds. There are only fragmentary data on their crystal structure [2, 6, 9] and optical properties [2, 4]. Data on their heat capacity or thermodynamic properties are not available in the literature. It is worth noting that, among the $RMGe_2O_7$ germanates, the high-temperature heat capacity and thermodynamic properties have been measured only for $YInGe_2O_7$ and $TmInGe_2O_7$ [11]. The phase diagram of the Eu_2O_3–Ga_2O_3–GeO_2 system has not yet been constructed. Thermodynamic modeling requires data on the thermodynamic properties of the compounds existing in this system, but such data are as yet not available.

The purpose of this work was to study the structure and thermophysical properties of $EuGaGe_2O_7$.

EXPERIMENTAL

Europium gallium germanate was prepared by solid-state reaction using Eu_2O_3 (reagent-grade), Ga_2O_3 (extrapure-grade), and GeO_2 (99.999%) as starting chemicals. After calcination at 1173 K, a stoichiometric oxide mixture was homogenized by grinding in an agate mortar and pressed into pellets, which were then fired in air at 1273 K for 40 h, 1373 K for 100 h, and 1473 K for 60 h. To drive the solid-state reaction to completion, the pellets were reground every 20 h and the resultant powders were then repressed. In doing so, we took into account that relatively high solid-state synthesis temperatures could cause partial GeO_2 vaporization [12]. Because of this, the synthesis process was run in lidded crucibles. The synthesis time and the amount of excess GeO_2 were optimized using experimental data. The phase composition of the resultant samples was determined by X-ray diffraction on a Bruker D8 Advance diffractometer (CuK_α radiation)

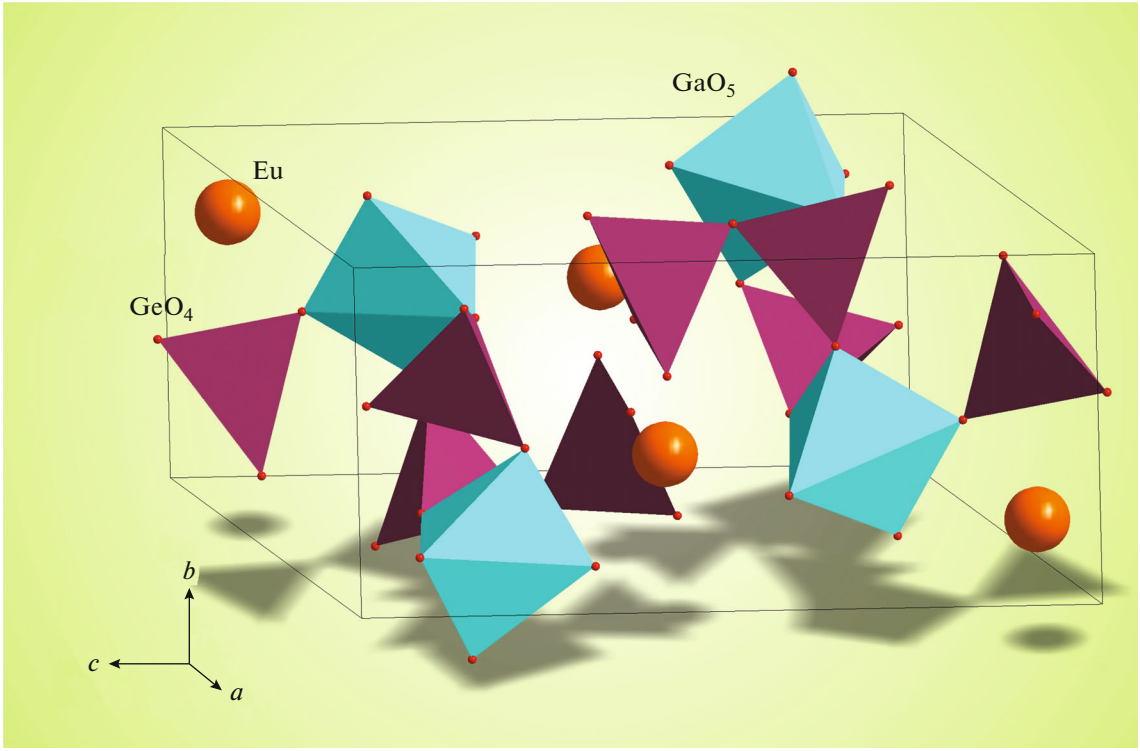

Fig. 1. Crystal structure of $EuGaGe_2O_7$.

equipped with a VANTEC linear detector (scan step, 0.016°; counting time per data point, 2 s).

The heat capacity of $EuGaGe_2O_7$ was measured using an STA 449 C Jupiter thermoanalytical system (Netzsch, Germany). The experimental procedure was described in detail elsewhere [13]. The uncertainty in our measurements was within 2%.

Table 1. Principal intensity data collection and structure refinement parameters for the $EuGaGe_2O_7$ compound (sp. gr. $P2_1/c$)

a, Å	7.16932(7)
b, Å	6.57008(6)
c, Å	12.7699(1)
β, deg	117.4522(5)
V, Å^3	533.768(8)
Z	4
d, g/cm^3	5.96
2θ range, deg	10–120
R_{wp}, %	1.87
R_p, %	1.48
R_{exp}, %	1.56
χ^2	1.20
R_B, %	0.43

a, b, c, and β are the unit-cell parameters; V is the unit-cell volume; d is the calculated density; R_{wp}, R_p, R_{exp}, and R_B are the weighted profile, profile, expected, and Bragg agreement factors, respectively; and χ^2 is the goodness-of-fit index.

RESULTS AND DISCUSSION

In structure refinement, we used TOPAS 4.2 software [14]. Almost all observed peaks could be indexed in a monoclinic structure ($P2_1/c$) with unit-cell parameters similar to those of $GdGaGe_2O_7$ [2]. Because of this, the structure of this compound was taken as an input model for refinement. For conversion, the Gd site was replaced by a Eu ion (Fig. 1). The thermal parameters of all the atoms were refined in an isotropic approximation. Refinement proceeded smoothly and converged to small R factors (Fig. 2, Table 1). The atomic position coordinates and principal bond lengths are presented in Tables 2 and 3, respectively.

The unit-cell parameters obtained by us for $EuGaGe_2O_7$ (Table 1) agree rather well with those reported by Kaminskii et al. [2]: a = 7.16(1) Å, b = 6.56(1) Å, c = 12.77(1) Å, β = 117.4(2)°, d = 5.98 g/cm^3.

Figure 3 illustrates the effect of temperature on the heat capacity of $EuGaGe_2O_7$. As the temperature is raised from 350 to 1053 K, its C_p rises systematically, without any extrema in the $C_p(T)$ curve. The present data can be represented by the Maier–Kelley equation [15]:

$$C_p = a + bT - cT^{-2}. \quad (1)$$

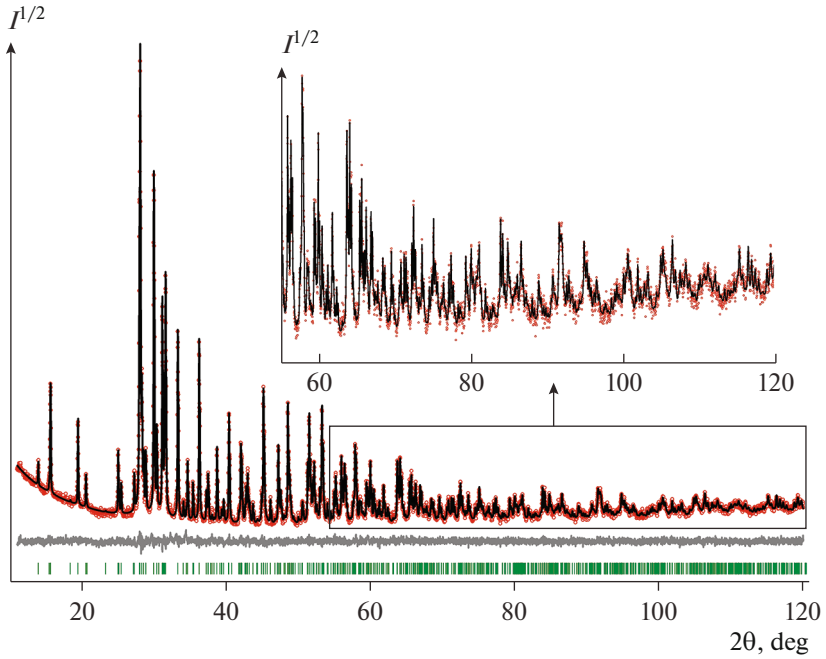

Fig. 2. Raw X-ray diffraction data, calculated profile, and difference plot for $EuGaGe_2O_7$.

For $EuGaGe_2O_7$, it has the following form:

$$C_p = (259.40 \pm 0.81) + (30.94 \pm 0.80) \times 10^{-3} T - (51.51 \pm 0.92) \times 10^5 T^{-2}. \quad (2)$$

The correlation coefficient for Eq. (2) is 0.9987 and the maximum deviation of the data points from the corresponding smoothed curve is 0.79%.

The present heat capacity data cannot be compared to other results because no such data are available in the literature. Note only that partial gallium substitution for europium leads to lower C_p values (Fig. 3).

The 298-K C_p of $EuGaGe_2O_7$ evaluated using the Neumann–Kopp equation [17]

$$C_{p,298}(EuGaGe_2O_7) = \frac{1}{2} C_{p,298}(Eu_2O_3) + \frac{1}{2} C_{p,298}(Ga_2O_3) + 2C_{p,298}(GeO_2) \quad (3)$$

is 213.7 J/(mol K). It follows from Eq. (2) that $C_{p,298}(EuGaGe_2O_7)$ = 210.57 J/(mol K). Thus, the heat capacity calculated using the Neumann–Kopp equation approaches the experimentally determined value (Δ = +1.2%). In the calculation by Eq. (3), we used the heat capacities of Eu_2O_3, Ga_2O_3, and GeO_2 borrowed from Leitner et al. [17]. The Kumok increment method [18] gives a slightly larger difference in C_p: Δ = +3.1%.

Using Eq. (2) in combination with well-known thermodynamic relations, we evaluated the thermodynamic functions (enthalpy increment, entropy change, and reduced Gibbs energy change) of the

Table 2. Atomic position coordinates and isotropic thermal parameters (B_{iso}) in the structure of $EuGaGe_2O_7$

Atom	x	y	z	B_{iso}
Eu	0.7608(2)	0.14629(18)	0.02552(11)	0.12(15)
Ga1	0.7897(3)	0.3998(4)	0.26951(16)	0.19(15)
Ge1	0.7836(4)	0.6578(4)	0.0437(2)	0.21(16)
Ge2	0.2995(4)	0.4120(4)	0.2216(2)	0.39(16)
O1	0.5905(17)	0.8253(17)	0.0223(8)	0.51(19)
O2	0.7818(14)	0.1114(18)	0.2136(9)	0.51(19)
O3	0.5697(15)	0.3753(18)	0.3099(9)	0.51(19)
O4	0.0010(16)	0.3372(18)	0.4206(9)	0.51(19)
O5	0.7442(18)	0.0037(14)	0.4164(10)	0.51(19)
O6	0.7919(16)	0.4455(14)	0.1263(10)	0.51(19)
O7	0.1502(18)	0.1844(15)	0.1800(11)	0.51(19)

Table 3. Principal bond lengths (Å) in the structure of $EuGaGe_2O_7$

Eu–O1^{I}	2.428(10)	Ga1–O4^{VI}	1.869(10)
Eu–O1^{II}	2.309(8)	Ga1–O6	1.860(11)
Eu–O2	2.348(9)	Ga1–O7^{VII}	1.960(10)
Eu–O3^{III}	2.450(10)	Ge1–O1	1.689(9)
Eu–O4^{IV}	2.536(10)	Ge1–O4^{VII}	1.826(9)
Eu–O4^{V}	2.626(7)	Ge1–O5^{III}	1.823(11)
Eu–O5^{III}	2.705(10)	Ge1–O6	1.733(10)
Eu–O6	2.303(10)	Ge2–O2^{VII}	1.785(10)
Eu–O7^{VI}	2.583(10)	Ge2–O3	1.751(8)
Ga1–O2	2.017(12)	Ge2–O5^{VII}	1.732(11)
Ga1–O3	1.879(6)	Ge2–O7	1.772(10)

Symmetry code: $x, y-1, z$ (I); $-x+1, -y+1, -z$ (II); $x, -y+1/2, z-1/2$ (III); $-x+1/2, y-1/2, -z+1/2$ (IV); $x+1, -y+1/2, z-1/2$ (V); $x+1, y, z$ (VI); $-x+1, y+1/2, -z+1/2$ (VII).

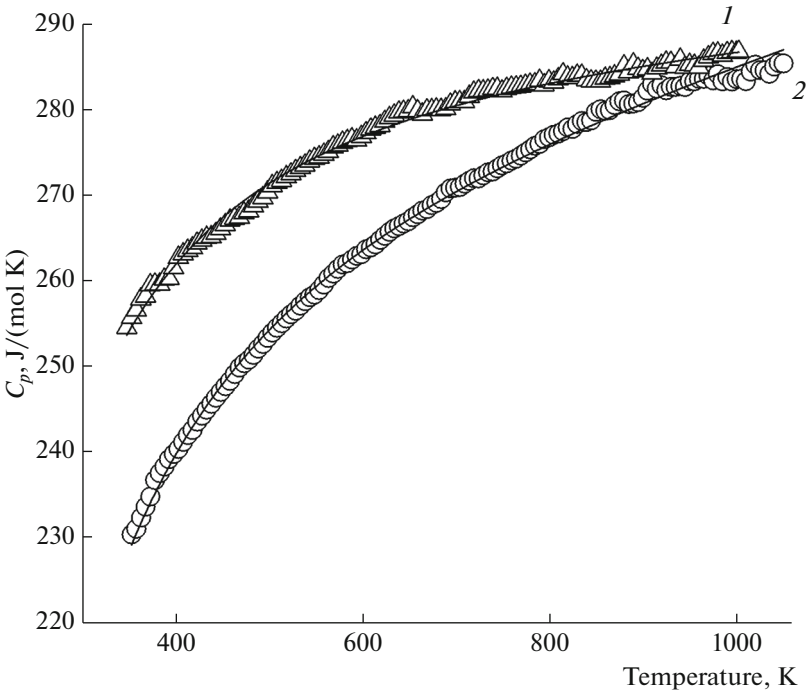

Fig. 3. Temperature dependences of molar heat capacity for (*1*) $Eu_2Ge_2O_7$ [16] and (*2*) $EuGaGe_2O_7$.

$EuGaGe_2O_7$ germanate. The results are presented in Table 4. It is seen that, above 750 K, the C_p values of the germanate exceed the classical Dulong–Petit limit $3Rs$, where R is the gas constant and s is the number of atoms per formula unit of the compound.

CONCLUSIONS

The $EuGaGe_2O_7$ germanate has been prepared by solid-state reaction and its crystal structure has been refined. Its high-temperature heat capacity has been determined by DSC in the temperature range 350–

Table 4. Thermodynamic properties of $EuGaGe_2O_7$

T, K	C_p, J/(mol K)	$H°(T) - H°(350\ K)$, kJ/mol	$S°(T) - S°(350\ K)$, J/(mol K)	$\Phi°(T)$, J/(mol K)
350	228.1	–	–	–
400	239.5	11.71	31.25	1.98
450	247.8	23.90	59.97	6.85
500	254.2	36.46	86.42	13.50
550	259.3	49.30	110.9	21.26
600	263.6	62.38	133.6	29.69
650	267.3	75.65	154.9	38.51
700	270.5	89.10	174.8	47.54
750	276.1	102.7	193.6	56.66
800	278.5	116.4	211.3	65.78
850	280.8	130.3	228.1	74.84
900	283.0	144.3	244.1	83.80
950	283.0	158.4	259.4	92.65
1000	285.1	172.6	273.9	101.3

1050 K. The $C_p(T)$ data have been shown to be well represented by the Maier–Kelley equation. The experimental $C_p(T)$ data have been used to calculate the thermodynamic properties of $EuGaGe_2O_7$.

REFERENCES

1. Jarchow, O., Klaska, K.-H., and Schenk, H., $REAlGe_2O_7$ – new compounds of rare earth germinates, *Naturwissenschaften,* 1981, vol. 68, pp. 475–476.
2. Kaminskii, A.A., Mill, B.V., Butashin, A.V., et al., Germanates with $NdAlGe_2O_7$-type structure. Synthesis, crystal structure, absorption–luminescence properties, and stimulated emission of their activator, Nd^{3+} ions, *Phys. Status Solidi A,* 1987, vol. 103, pp. 575–592.
3. Cascales, C., Puebla, G., Klimin, S., et al., Magnetic ordering in the rare earth iron germanates $HoFeGe_2O_7$ and $ErFeGe_2O_7$, *Chem. Mater.,* 1999, vol. 11, pp. 2520–2526.
4. Lozano, G., Cascales, C., Zaldo, C., and Porcher, P., Measurement and simulation of the energy levels of $R = Pr^{3+}$ and Nd^{3+} in $GaRGe_2O_7$, *J. Alloys Compd.,* 2000, vols. 303–304, pp. 349–354.
5. Kaminakii, A.A., Rhee, H., Lux, O., et al., Monoclinic $LaGaGe_2O_7:Nd^{3+}$ – a novel SRS- and SE-active crystal with high-order Stokes and anti-Stokes picosecond $\chi^{(3)}$-nonlinear lasing, *Laser Phys. Lett.,* 2013, vol. 10, paper 075 803. https://doi.org/10.1088/1612-2011/10/7/075803
6. Jarchow, O., Klaska, K.-H., and Schenk-Strauß, H., Die Kristallstrukturen von $NdAlGe_2O_7$ und $NdGaGe_2O_7$, *Z. Kristallogr.,* 1985, vol. 172, pp. 159–166.
7. Cascales, C., Fernàndez-Diaz, M.T., Monge, M.A., and Bucio, L., Crystal structure and low-temperature magnetic ordering in rare earth iron germanates $RFeGe_2O_7$, R = Y, Pr, Dy, Tm, and Yb, *Chem. Mater.,* 2002, vol. 14, pp. 1995–2003. https://doi.org/10.1021/cm0111332
8. Buciot, L., Cascales, C., Alonso, J.A., and Rasines, I., Neutron diffraction refinement characterization of $FeRGe_2O_7$ (R = La, Pr, Nd, Gd), *J. Phys.: Condens. Matter,* 1996, vol. 8, pp. 2641–2653.
9. Juarez-Arellano, E.A., Campa-Molina, J., Ulloa-Godinez, S., et al., Crystallochemistry of thortveitite-like and thortveitite-type compounds, *Mater. Res. Soc. Symp.,* 2005, vol. 848, pp. FF6.15.1–FF6.15.8.
10. Denisova, L.T., Kargin, Yu.F., Irtyugo, L.A., et al., Heat capacity of $In_2Ge_2O_7$ and $YInGe_2O_7$ from 320 to 1000 K, *Inorg. Mater.,* 2018, vol. 54, no. 12, pp. 1245–1249. https://doi.org/10.1134/S0020168518120026
11. Denisova, L.T., Irtyugo, L.A., Belousova, N.V., et al., High temperature heat capacity and thermodynamic properties of $Tm_2Ge_2O_7$ and $TmInGe_2O_7$ in the region of 350–1000 K, *Russ. J. Phys. Chem. A,* 2019, vol. 93, no. 3, pp. 598–601. https://doi.org/10.1134/S003602441903004X
12. Becker, U.W. and Felsche, J., Phases and structural relations of the earth germanates $RE_2Ge_2O_7$, RE = La–Lu, *J. Less-Common Met.,* 1987, vol. 128, pp. 269–280.
13. Denisova, L.T., Irtyugo, L.A., Kargin, Yu.F., et al., High-temperature heat capacity and thermodynamic properties of $Tb_2Sn_2O_7$, *Inorg. Mater.,* 2017, vol. 53, no. 1, pp. 93–95. https://doi.org/10.1134/S0020168517010046
14. *Bruker AXS TOPAS V4: General Profile and Structure Analysis Software for Powder Diffraction Data. User's Manual,* Karlsruhe: Bruker AXS, 2008.
15. Maier, C.G. and Kelley, K.K., An equation for the representation of high temperature heat content data, *J. Am. Chem. Soc.,* 1932, vol. 54, no. 8, pp. 3243–3246.
16. Denisova, L.T., Irtyugo, L.A., Kargin, Yu.F., et al., Synthesis and High-Temperature Heat Capacity of $Sm_2Ge_2O_7$ and $Eu_2Ge_2O_7$, *Inorg. Mater.,* 2018, vol. 54, no. 2, pp. 167–170. https://doi.org/10.1134/S0020168518020048
17. Leitner, J., Chuchvalec, P., Sedmidubský, D., et al., Estimation of heat capacities of solid mixed oxides, *Thermochim. Acta,* 2003, vol. 395, nos. 1–2, pp. 27–46.
18. Kumok, V.N., Problem of matching techniques for evaluating thermodynamic characteristics, in *Pryamye i obratnye zadachi khimicheskoi termodinamiki* (Direct and Inverse Problems in Chemical Thermodynamics), Novosibirsk: Nauka, 1987, pp. 108–123.

Translated by O. Tsarev